10-4-2017

Silver Engineered Nanomaterials and Ions Elicit Species-Specific O_2 Consumption Responses in Plant Growth Promoting Rhizobacteria

Ricky W. Lewis
University of Kentucky, rale243@uky.edu

Jason M. Unrine
University of Kentucky, jason.unrine@uky.edu

Paul M. Bertsch
University of Kentucky, paul.bertsch@uky.edu

David H. McNear Jr.
University of Kentucky, dave.mcnear@uky.edu

Right click to open a feedback form in a new tab to let us know how this document benefits you.

Follow this and additional works at: https://uknowledge.uky.edu/pss_facpub

Part of the Plant Sciences Commons, and the Soil Science Commons

Silver Engineered Nanomaterials and Ions Elicit Species-Specific O₂ Consumption Responses in Plant Growth Promoting Rhizobacteria

Silver engineered nanomaterials and ions elicit species-specific O$_2$ consumption responses in plant growth promoting rhizobacteria

Ricky W. Lewis[a] and Jason Unrine
Department of Plant and Soil Sciences, University of Kentucky, Lexington, Kentucky 405046

Paul M. Bertsch
Department of Plant and Soil Sciences, University of Kentucky, Lexington, Kentucky 405046; CSIRO Land and Water, 41 Boggo Road, Ecosciences Precinct, Dutton Park, Queensland 4102, Australia; and Center for the Environmental Implications of Nanotechnology (CEINT), Duke University, Durham, North Carolina 27708

David H. McNear, Jr.
Department of Plant and Soil Sciences, University of Kentucky, Lexington, Kentucky 405046

Metal containing engineered nanomaterials (ENMs) are now commonly used in various industrial and commercial applications. Many of these materials can be transformed during waste water treatment and ultimately enter terrestrial ecosystems via agriculturally applied biosolids. It is unclear how agriculturally important soil microbes will be affected by exposure to environmentally relevant, sublethal concentrations of ENMs and their transformation products (i.e., ions, aggregates, etc.). A method was developed, which puts O$_2$ consumption responses in terms of viability, and tested by examining the toxic effects of Ag$^+$, Zn^{2+}, and Ni^{2+} ions on the plant growth promoting rhizobacterium (PGPR) *Bacillus amyloliquefaciens* GB03. The method was then used to examine the toxicity of Ag$^+$, as-synthesized polyvinylpyrrolidone-coated silver ENM (PVP-AgENMs), and 100% sulfidized AgENM on *B. amyloliquefaciens* GB03, and two additional PGPRs *Sinorhizobium meliloti* 2011, and *Pseudomonas putida* UW4. *S. meliloti* was found to have the highest LC$_{50}$ for Ag$^+$ and PVP-AgENMs (6.6 and 207 μM, respectively), while *B. amyloliquefaciens* and *P. putida* exhibited LC$_{50}$'s for Ag$^+$ and PVP-AgENMs roughly half those observed for *S. meliloti*. The authors observed species-specific O$_2$ consumption responses to ENM and ion exposure. PVP-AgENMs were less toxic than ions on a molar basis, and abiotic dissolution likely explains a significant portion of the observed toxic responses. Our results suggest microbes may exhibit distinct metabolic responses to metal and ENM exposure, even when similar LC$_{50}$'s are observed. These findings together illustrate the importance of understanding species-specific toxic responses and the utility of examining O$_2$ consumption for doing so. © 2017 American Vacuum Society. https://doi.org/10.1116/1.4995605

I. INTRODUCTION

Engineered nanomaterials (ENMs), human designed and manufactured materials with at least one dimension between 1 and 100 nm,[1] are now widely utilized in an array of consumer and medical products, and industrial applications. The antimicrobial properties of silver have been exploited by humans for centuries, but silver containing ENMs (AgENMs) and other ENMs are currently entering commercial and municipal waste streams. It has been predicted the rate at which they will be deposited in terrestrial environments through biosolids amendment of agricultural soils will increase exponentially.[2] Debate remains regarding predicted environmental concentrations of ENMs, due in part to differences in models implemented to predict environmental concentrations and the lack of empirical data regarding them.[2–5] While biosolids amended soils are predicted to have low μg/kg to mg/kg concentrations of AgENMs in the near term,[2,5] observed concentrations of total silver in biosolids can vary greatly and have been observed as high as ∼856 mg Ag/kg dry biosolids.[4]

Despite the debate regarding concentrations of AgENMs in the environment, their exponential rate of release alone constitutes an urgent need to explore the response of relevant test organisms to AgENM exposure. One such group of relevant test organisms is those bacteria inhabiting the dynamic and nutrient rich 1–2 mm zone around a plant root (a.k.a. the rhizosphere) which have been shown to have significant ecological and agricultural benefits. While the effects of AgENMs (and other ENMs) on beneficial soil bacteria and other soil microbes remain largely neglected, interest is steadily growing.[3]

Most microbial nanotoxicology studies have focused primarily on "pristine" or "as manufactured" ENMs.[3,6] However, ENMs undergo various transformations during the wastewater treatment process and after application to soils which can lead to, for example, sulfidation (the formation of sulfides) and reduced toxicity of AgENMs.[6–8] Additionally, few nanotoxicological studies focus on integrative physiological responses, such as O$_2$ consumption. This is crucial because a range of toxic responses can occur prior to cell death, and antibiotic efficacy has recently been linked to modulation of respiration in medically relevant microbes.[9]

a)Electronic mail: ricky.w.lewis@gmail.com

Respiration may also sometimes be a useful endpoint when examining metal/nanomaterial induced stress in microbes.[10–12]

The first experiment in this paper (experiment 1) demonstrates a high-throughput O$_2$ consumption and viability assay that was developed and tested by assessing the response of *Bacillus amyloliquefaciens* GB03 (formerly *Bacillus subtilis* GB03) to Zn^{2+}, Ni^{2+}, and Ag$^+$ ions along with streptomycin controls (experiment 1). *B. amyloliquefaciens* GB03 is a relatively rapidly growing Gram-positive bacterium utilized as a fungicide[13] which promotes plant growth.[14] Silver was chosen because its toxic effects are well documented and intracellular concentrations are not tightly regulated, whereas Zn^{2+} and Ni^{2+} were chosen because they are regulated essential nutrients that are also toxic at elevated concentrations and both have been shown to display toxicity to *B. subtilis* (a relative of *B. amyloliquefaciens*) at similar concentrations under the same test conditions.[15] Additionally, mechanisms governing intracellular Zn^{2+} concentrations are relatively well understood, while less is known regarding Ni^{2+} homeostasis.

In experiment 2, the method was used to evaluate O$_2$ consumption and viability of *B. amyloliquefaciens* GB03 and two additional agriculturally and ecologically relevant plant growth promoting rhizobacteria (PGPR), *Sinorhizobium meliloti* 2011 and *Pseudomonas putida* UW4, exposed to Ag$^+$ ions, untransformed polyvinylpyrrolidone-coated AgENM (PVP-AgENMs), and 100% sulfidized PVP-AgENMs (sAgENMs). *S. meliloti* 2011 is a relatively slow growing Gram-negative bacterium capable of forming a nitrogen-fixing symbiosis with the model legume, *Medicago truncatula*, and related strains are known to promote lettuce growth.[16] Additionally, nodulation of *M. truncatula* A17 by *S. meliloti* 2011 was inhibited by biosolids enriched with nanoscale Ti, Zn, and Ag.[17] *P. putida* UW4 is a rapidly growing gram-negative bacterium capable of plant growth promotion and protection against many environmental/pathogen stresses, likely through modulation of plant physiology via the production of 1-aminocyclopropane-1-carboxylic acid deaminase.[18] While various strains of *P. putida* have been the subject of many nanotoxicological studies, no study to date has reported the response of UW4 to nanomaterials.

II. METHODS

Toxicity was assessed by first measuring O$_2$ consumption during exposure to metals or antibiotics followed by regrowth of the cells. Experiment 1 was performed to develop a high-throughput method of assessing O$_2$ consumption and viability responses (Table I). In this experiment, we examined the toxicity of Ag$^+$, Zn^{2+}, and Ni^{2+} to *B. amyloliquefaciens*. Experiment 2 was performed on a different microplate reader and the same calibrations and standard (streptomycin) was used in both experiments. In this experiment *B. amyloliquefaciens*, *P. putida*, and *S. meliloti* were exposed to Ag$^+$, PVP-AgENMs, and sAgENMs. Highly detailed methods are available in the supplementary material.[49]

A. Maintenance and isolation of bacteria

B. amyloliquefaciens GB03, *S. meliloti* 2011, and *P. putida* UW4 cultures were made from 1:1 [glycerol:tryptone–yeast (TY) extract-culture] stocks by streaking on 1% TY agar plates and incubating at 28 °C. For each experimental repeat (block), a single colony was inoculated into TY + 50 mM 2-morpholin-4-ylethanesulfonic acid (MES) (pH = 6) medium and cultured to midlate log phase (OD$_{600\,nm}$ ∼ 0.6–0.86) at 28 °C. Cells were then isolated to the desired cell density (OD$_{600\,nm}$ ∼ 1–1.2) by washing in 50 mM MES three times before use in calibration and exposure procedures.

B. Exposure procedure

One hour before exposure, 50 μl of 50 mM MES was transferred to each well of an Oxoplate^{TM} to pre-equilibrate the plate. To initiate exposure, either 100 μl of the live cell suspension or 50 mM MES was transferred to each designated well of the Oxoplate. Twenty five microliters of 8× concentrated metal solutions (in 50 mM MES) were then added to each well, followed by 25 μl of 10% glucose + 50 mM MES. The plate was then sealed with a clear, sterile polymerase chain reaction (PCR) film, and fluorescence intensity was measured over time for an O$_2$ sensitive indicator dye (excitation: 540 nm, emission: 650 nm) and a reference dye (excitation: 540 nm, emission: 590 nm). O$_2$ consumption curves were generated using the fluorescence intensity measurements and the Oxoplate supplier's instructions. After 1.5 h, cells were diluted 500× to a total of 100 μl in a clear, sterile 96 well plate. Then, 100 μl of 2× TY + 50 mM MES (pH = 6) was transferred to each well, the plate was sealed with a clear, sterile PCR film, and cell growth was monitored by measuring absorbance over time. In experiment 1, a Wallac Victor 2 microplate reader

TABLE I. Outline of experiments. PVP-AgENM = untransformed polyvinylpyrrolidone-coated silver engineered nanomaterial, sAgENM = 100% sulfidized silver engineered nanomaterial. Test organism(s) and metals are the bacteria and metals used in toxicity assays.

Experiment	Test organism(s)	Metals	Experimental goals
1	*B. amyloliquefaciens* GB03	Ag$^+$, Zn^{2+}, Ni^{2+}	Develop a high-throughput method of assessing O$_2$ consumption and viability in aerobic bacteria. Assess the toxicity of Ag$^+$, Zn^{2+}, Ni^{2+} to *B. amyloliquefaciens*
2	*B. amyloliquefaciens* GB03 *S. meliloti* 2011 *P. putida* UW4	Ag$^+$, PVP-AgENM, sAgENM	Assess the toxicity of Ag$^+$, PVP-AgENM, sAgENM to *B. amyloliquefaciens*, *S. meliloti*, and *P. putida*. Compare O$_2$ consumption responses across species

(Perkin-Elmer Life Sciences, MA) was used and spectral interference inherent to the system was overcome by generating growth curves by using a dual-wavelength method (absorbance$_{450-600\,nm}$ = absorbance$_{450\,nm}$ − absorbance$_{600\,nm}$). In experiment 2, a Spectramax i3 microplate reader (Molecular Devices, Wokingham, UK) was used, and no spectral interference was detected, so growth curves were generated from a single absorbance wavelength (600 nm).

C. O_2 consumption and viability assay calibration

To assess O_2 consumption and regrowth as percentages of an unexposed control, it was necessary to calibrate the O_2 consumption and viability assays (Fig. 1). A sham exposure (without metals or antibiotics) was performed as in Sec. II B. Prior to the sham exposure, cells were diluted to known cell density proportions before being loaded into the Oxoplate. The O_2 partial pressure (in terms of percent air saturation) per well over time (1.5 h) was measured using the methods described by the Oxoplate manufacturer. O_2 consumption curves (percent air saturation over time) were generated for each well, and regression was used to determine the relationship between starting cell density and area under the O_2 consumption curves (Fig. 1).

After the O_2 consumption calibration was complete, cells were diluted 1000× and regrowth was monitored using absorbance as described in Sec. II B. Growth curves were related to starting cell density by recording the time at which cells in each well reached exponential growth and regressing this time against the starting cell density, which is similar to techniques used by others.[19,20] Because initiation of exponential growth was determined via growth curves, it was necessary to test absorbance thresholds to ensure a good relationship between starting cell density and the time at which a growth curve passes a particular absorbance threshold (Fig. 1).

D. Experimental design and data analysis

In experiment 1, a randomized complete block design (RCBD) was used to evaluate the toxicity of Ag^+ (0.5, 1, 2, 3, 4, 6, 8, and 10 μM), Ni^{2+}, and Zn^{2+} (0.63, 1.3, 2.5, 5, 10, 20, 40, and 80 μM) to *B. amyloliquefaciens* using seven experimental blocks. A metal free control was also used across all experimental blocks. Treatments were randomized by column, and control columns were randomized by row across all experimental blocks. Technical replicates of each treatment were performed in triplicate in each experimental block. Ions were supplied as $AgNO_3$, $ZnSO_4$, or $NiSO_4$.

Distribution and variance of residuals were determined following linear regression using distribution plots, Q-Q plots, and Studentized residual plots. Treatment responses were normalized to metal free control wells, averaged within experiments, and the average of experimental means were compared to a hypothetical mean (H_O: $\mu = 100\%$, for viability and O_2 consumption measurements) using a two-tailed, one-sample *t*-test (n = 7, alpha = 0.05, assuming unequal

variances). Mean O_2 consumption responses of each experiment were plotted against mean viability measurements and regression curves were fit using SOFTMAX PRO 6.4 (Molecular Devices, Wokingham).

In experiment 2, an RCBD was used to assess toxicity in *B. amyloliquefaciens*, *P. putida*, and *S. meliloti*, with three experimental blocks and three replicates per block with randomization as in experiment 1. *B. amyloliquefaciens* and *S. meliloti* were exposed to 2.6 μM streptomycin, $AgNO_3$ (0.5, 1, 2, 3, 4, 5, 6, and 10 μM), 296 μM sAgENM, and PVP-AgENM (4.6, 37, 55.6, 111, 148, 185, 222, and 296 μM). The same concentrations of $AgNO_3$, streptomycin, and sAgENM, but 4.3, 34.5, 43, 46, 115, 144, 172, and 230 μM PVP-AgENM were used for *P. putida* exposures. Molarity is expressed in terms of total silver concentration. Viability and O_2 consumption estimates were normalized to the no metal controls and were found to be non-normally distributed. The data were ranked and analysis of variance was used to examine experiment by treatment interactions. Because no experiment by treatment interactions were found, observations were pooled across experiments (n = 9) and a two-tailed Wilcoxon signed rank test was used to compare the observations to a hypothetical mean of 100% viability or O_2 consumption (H_0: $\mu = 100\%$, α 0.05) using JMP®, Version 12, SAS Institute Inc., Cary, NC, 1989-2007.

Sigmaplot was used to generate nonlinear, four-parameter dose response curves and extrapolate LC_{50} values for viability responses to PVP-AgENM and $AgNO_3$. LC_{50} values were compared using an unpaired *t*-test with a Bonferroni correction. Additionally, Sigmaplot was used to perform regression analyses on O_2 consumption-viability plots for interpreting O_2 consumption responses in terms of relative viable cell numbers. Dissolution measurements were used to generate predicted viability responses to the dissolved fraction of AgENMs by extrapolating responses from $AgNO_3$ dose response curves for the average dissolution estimate ± one standard deviation (n = 3).

E. Metal and ENM characterization

Concentrations of stock metals were determined via inductively coupled plasma mass spectrometry (ICP-MS) analysis prior to exposure. PVP-AgENMs and sAgENMs were characterized in the exposure medium at $\sim$300 μM total silver and 28 °C using a Zetasizer Nano ZS (Malvern). Hydrodynamic diameter and electrophoretic mobility were estimated using direct light scattering and electrophoretic light scattering, respectively. The particles used were previously characterized and PVP-AgENMs had a primary particle size of 53–58 nm,[21,22] while sAgENMs had a primary particle size of $\sim$65 nm,[21] both determined via transmission electron microscopy.

A sham exposure (without bacteria) was performed to examine the abiotic dissolution of PVP-AgENMs and sAgENMs in the exposure medium. Briefly, PVP-AgENM (29, 115, and 230 μM) and sAgENM ($\sim$300 μM) were

Calibration/exposure workflow diagram
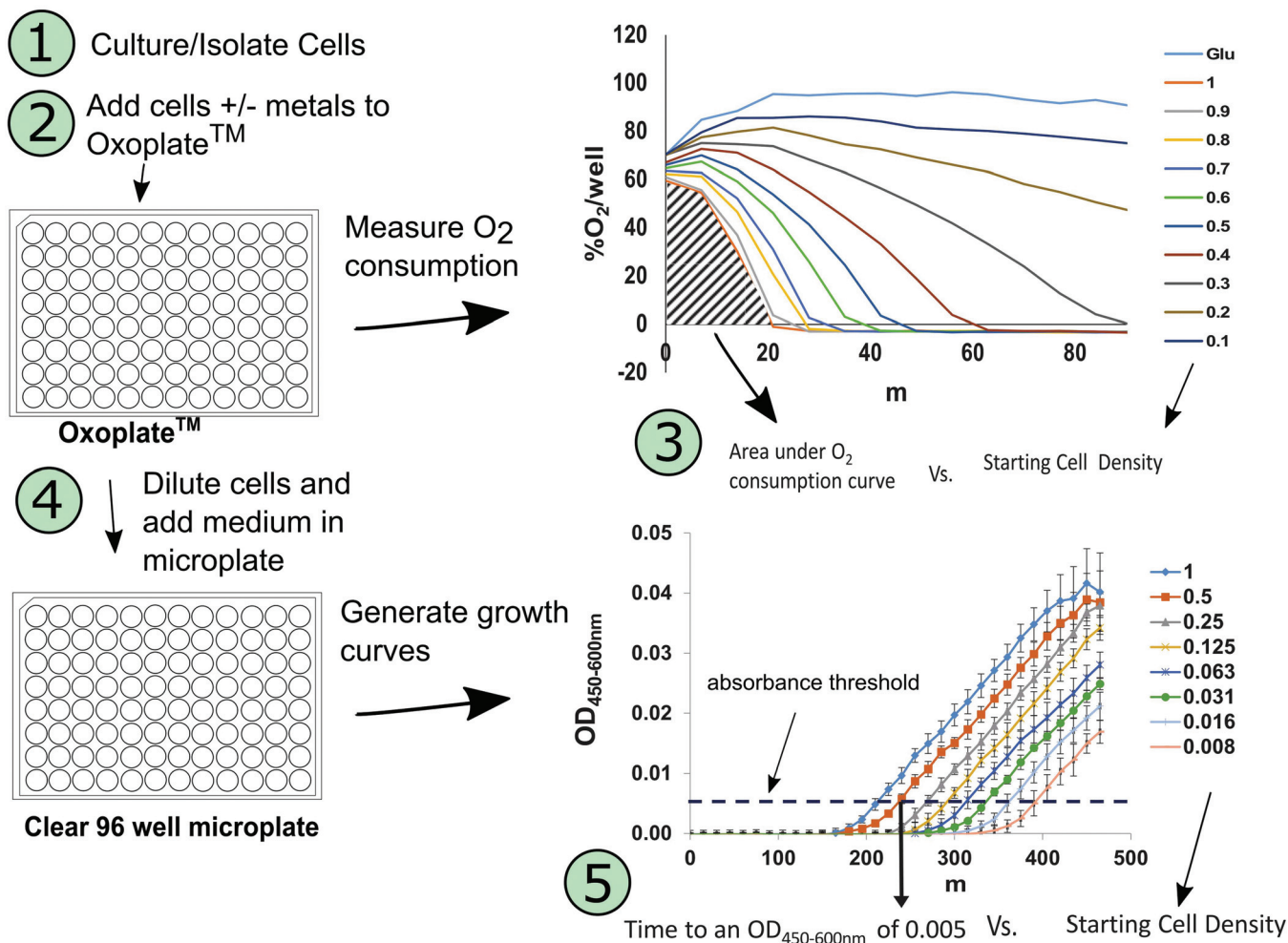
1) Culture, Isolate, and Dilute Cells
   a) For calibration, dilute to known cell densities
2) Load cells into Oxoplate
   a) Add glucose (for exposures, add metals + glucose)
   b) Measure O_2 concentration over time
3) Measure area under O_2 consumption curve
   a) Relate area under curve to starting cell density
4) Dilute cells and load into clear 96 well plate
   a) Add medium and monitor growth
5) Measure time to absorbance threshold (dotted line)
   a) Relate time to absorbance threshold to starting cell density

Note: After calibration curves are generated, area under the curve
and time to absorbance threshold can be used to caclulate % O_2
consmption and % Viability, respectively, of cells exposed to metals, etc.

Fig. 1. Workflow diagram of the calibration/exposure procedures. Circled numbers indicate step of the process (listed at the bottom of the figure).

prepared in the exposure medium with glucose and brought to 2 ml in ultracentrifuge tubes. Samples were gently vortexed to ensure mixing and 100 μl was immediately removed for total metal analysis, before centrifuging for 90 m at 28 °C and 246 000g. According to Stoke's law, these conditions were sufficient to sediment spherical particles $\geq$2 nm. After centrifugation, 1 ml was removed and acidified to 1% HCl for dissolved metal analysis. Samples for total metal analysis were microwave digested at 100 °C and 400 W for 35 m (20 m ramp, 10 m hold, 5 m cooldown) in 13% HCl/40%
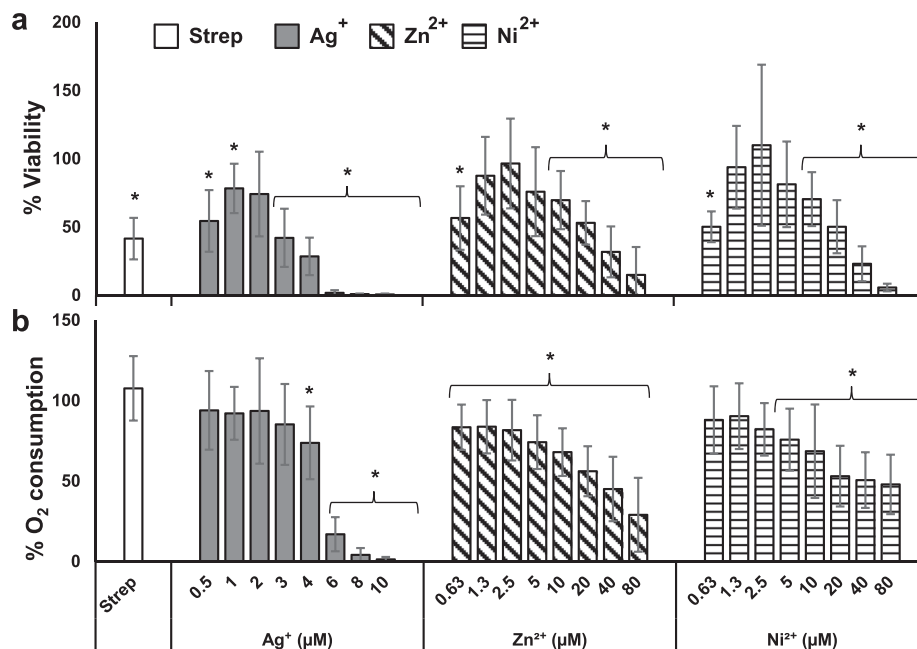
FIG. 2. Response of *Bacillus amyloliquefaciens* GB03 to Ag^+, Zn^{2+} and Ni^{2+} metal ions. (a) Percent viable cells after exposure. (b) Percent O_2 consumption over the course of exposure. All bars are standard deviation of seven experiments, * indicates response is statistically different from hypothetical mean (H_O: $\mu = 100\%$ for viability and respiration measurements) as determined using a two-tailed, one-sample *t*-test at alpha 0.05, assuming unequal variance.

HNO_3 before diluting 15 times in double deionized water, yielding 1% HCl/3% HNO_3. Metal concentrations were determined using an Agilent 7500 series ICP-MS (Santa Clara, CA).

F. Chemical equilibrium modeling

In experiment 1, exposure media were modeled using Geochem-EZ (Ref. 23) to determine the free ion activities of the metals of interest (Figs. S1 and S2). It was necessary to update the ligand database to include stability constants for Zn-MES (Ref. 24) and Ni-MES complexes.[24,25] The stability constant for the Ag-MES complex was approximated with the published stability constant for Ag-taurine complexes found using the International Union of Pure and Applied Chemistry Stability Constant Database.[26] All stability constants were input at infinite dilution. After concentrations of exposure media constituents were entered into Geochem-EZ, *p*H was fixed at 6, precipitates were allowed to form, and the ionic strength was calculated using an initial "guess" of 0.01 mol, as recommended by the model developers. In experiment 2, free ion concentrations and activities of Ag^+ from $AgNO_3$ or the expected dissolved silver from AgENMs were modeled using GeoChem-Ez,[23] as in experiment 1.

III. RESULTS AND DISCUSSION

A. Experiment 1: O_2 consumption by viability assays were effective at detecting the response of *B. amyloliquifaciens* to sublethal metal concentrations

1. Bacillus amyloliquefaciens response to Ag^+ ions

There were statistically significant reductions in oxygen consumption per well in the 4, 6, 8, and 10 μM Ag^+

exposures [Fig. 2(b)]. Normalizing these responses to viable cells revealed large overall increases in oxygen consumption per viable cell in response to Ag^+ exposure [Fig. 3(a)]. A four-parameter nonlinear curve yielded an $R^2 = 0.895$, implying O_2 consumption and viability correlate in a
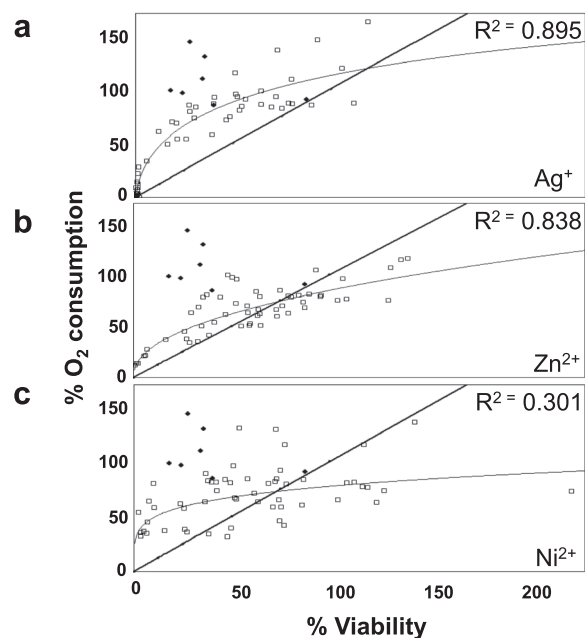

FIG. 3. Regression plots of percent O_2 consumption vs percent viability for *Bacillus amyloliquefaciens* GB03. (a) Ag^+ (open boxes), (b) Zn^{2+} (open boxes), and (c) Ni^{2+} (open boxes). Black diamonds in all plots are the response in each experiment to streptomycin. Using SOFTMAX PRO 6.4, a four-parameter curve was fit to the Ag^+ induced responses and log-log curves were fit to the Zn^{2+} and Ni^{2+} induced responses.

nonlinear manner in response to silver ions. Only ~30% of the cells were viable after exposure to 4 μM Ag$^+$ [Fig. 2(a)] and there was nearly complete mortality after exposure to 8–10 μM Ag$^+$ [Fig. 2(a)]. Cell viability was reduced following exposure to all tested Ag$^+$ concentrations, although the response at 2 μM was not significant ($p = 0.07$) [Fig. 2(a)].

Exposure of *Escherichia coli* to Ag$^+$ concentrations similar to those in this study (<10 μM) has been shown to stimulate respiration in the presence and absence of glucose.[27] The authors suggest this is due to uncoupling of the electron transport chain, which may at least partly explain the respiration responses to Ag$^+$ we observed. Jin *et al.*[28] found the IC$_{50}$ for Ag$^+$ and Ag nanoparticles to be highly dependent on the presence of specific ions for both *B. subtilis* and *P. putida*, with the Ag$^+$ 24 h IC$_{50}$ for *B. subtilis* ranging from <1 to ~18 μM, Suresh *et al.* found ~73 μM Ag$^+$ completely inhibited growth of *B. subtilis* (ATCC 9372) in Luria-Bertani (LB) medium,[29] while Kim *et al.* found ~463 μM Ag$^+$ was required to completely inhibit the growth of *B. subtilis* (KACC10111) in LB medium.[30] Our results show that relatively low concentrations of Ag$^+$ are toxic to *B. amyloliquefaciens* in the minimal exposure medium used this study [Fig. 2(a)].

2. Bacillus amyloliquefaciens response to Zn^{2+} ions

There was a decrease in O$_2$ consumption per well in response to all Zn^{2+} concentrations tested [Fig. 2(b)]. The O$_2$ consumption-viability plots showed increased O$_2$ consumption when percent viability was low and decreased O$_2$ consumption when viability was high [Fig. 3(b)]. A log-log regression was used to generate a nonlinear curve (R^2 of 0.838), supporting the notion that a nonlinear relationship exists between O$_2$ consumption and viability responses to Zn^{2+}. A statistically significant decrease in viability was induced by 0.63 and 10–80 μM Zn^{2+}, with viability gradually declining with increasing [Zn^{2+}] [Fig. 2(a)]. We found only ~15% of *B. amyloliquefaciens* cells exposed to 80 μM Zn^{2+} remained viable after exposure [Fig. 2(a)].

Previously, 1.8 mM Zn^{2+} was found to completely inhibit growth of *B. subtilis* WT, while 1 mM Zn^{2+} led to only a 20% reduction in optical density (600 nm).[15] Additionally, Kim and An[31] found colony forming units (CFU) counts of *B. subtilis* KACC10111 were significantly reduced (~40% of the control) in response to 1 mM Zn^{2+}. Van Nostrand *et al.*[32] found a 64% reduction in growth of *Burkholderia cepacia* PR1$_{301}$ exposed to 3.8 mM Zn^{2+} at pH 6. It is also worth noting that a meta-analysis examining the toxicity of nanoparticles and associated ions to environmentally relevant test organisms estimated the average MIC of Zn^{2+} to be ~459 μM.[33] Relative to these studies, we observed responses to low Zn^{2+} concentrations in *B. amyloliquefaciens*.

3. Bacillus amyloliquefaciens response to Ni^{2+} ions

While a gradual decline in O$_2$ consumption per well was observed in response to 2.5–80 μM Ni^{2+} [Fig. 2(b)], the O$_2$ consumption-viability plots showed high variability in O$_2$

consumption in terms of viability [Fig. 3(c)]. In fact, a log–log regression showed a nonlinear correlation between O$_2$ consumption and viability, but an R^2 value of 0.301 indicates this is a relatively weak correlation. Statistically significant declines in cell viability were observed in response to 0.63 μM Ni^{2+} and for 10–80 μM Ni^{2+} [Fig. 2(a)].

Gaballa and Helmann[15] reported 1.8 mM Ni^{2+} or Zn^{2+} were required to completely inhibit growth of *B subtilis* WT. We also found responses to Zn^{2+} and Ni^{2+} were similar in terms of O$_2$ consumption per well and viability in *B. amyloliquefaciens* (Fig. 2); however, the O$_2$ consumption-viability plots show a difference in the respiration response induced by these metals (Fig. 3). Modeling the exposure solutions showed, at equal total molar concentrations, the estimated concentration and activity of free Ni^{2+} were greater than that of Zn^{2+}, due Zn-MES interactions (Fig. S1). The higher free ion activity of Ni^{2+} may be partially responsible for the difference we found in O$_2$ consumption-viability relationships compared with Zn^{2+}; however, the relationship between O$_2$ consumption and viability was weakly correlated under Ni^{2+} exposure and not Zn^{2+}, suggesting a different biological response to the metals.

4. Bacillus amyloliquefaciens response to streptomycin

When compared with the no-metal/antibiotic control, 2.6 μM streptomycin significantly decreased the number of viable cells (~40%), while having no significant influence on O$_2$ consumed per well (Fig. 2). Expressing the respiration response relative to viable cells shows elevated O$_2$ consumption per cell of *B. amyloliquefaciens* exposed to streptomycin (Fig. 3). This response is of interest because accelerated respiration in response to sublethal antibiotic concentrations has recently been shown to potentiate bactericidal lethality of a range of antibiotics,[9] select for antibiotic resistant bacteria, or increase mutagenesis.[34]

B. Experiment 2: Response of PGPRs to ENMs

1. Assay calibration and ENM characterization

We observed mortality of *P. putida* in the Oxoplate when OD$_{600 nm}$ was 1.191 (before dilution in the Oxoplate); this was the greatest cell density used in the initial calibration curves, so this point was removed from the curve (Table S1). At cell densities similar to those used in the exposure conditions, *P. putida* exhibited no significant change in cell viability (Table S1). *S. meliloti* showed modest levels of growth during the O$_2$ consumption assay. We found strong correlations between starting cell density and time to OD$_{600 nm}$ of 0.09 in viability assays, and between starting cell density and the area under the curve in O$_2$ consumption assays (Table S2). Hydrodynamic diameter and electrophoretic mobility of PVP-AgENMs and sAgENMs were stable in the exposure medium over the course of the study, and in the absence of bacteria (Table II). Dissolution of sAgENM was minimal (0.14% ± 0.02), while dissolution of PVP-AgENM was moderate (6.15% ± 0.23, error is one standard deviation).

TABLE II. Characterization of PVP-AgENM and sAgENM particles in exposure medium using dynamic light scattering and electrophoretic light scattering at 0 and 90 min. PVP-AgENM, polyvinylpyrrolidone-coated silver ENM (primary particle size = 53–58 nm); sAgENM, 100% sulfidized AgENM (primary particle size = 65 nm); z-avg d. (nm), average intensity weighted hydrodynamic diameter in nanometers; μm cm V s, electrophoretic mobility; SD, one standard deviation; m, minutes. Diameter and electrophoretic mobility values are averages of 3 replicates. Significant differences were evaluated at α 0.05 as determined via a Studentized *t*-test comparing measurements at 0 and 90 m, no differences were observed.

Engineered nanomaterial (ENM)	Time (m)	Hydrodynamic diameter [Z-avg d. nm ($\pm$ SD)]	Electrophoretic mobility [μm cm/V s ($\pm$ SD)]
PVP-AgENM	0	84.6 ($\pm$0.9)	−0.24 ($\pm$0.1)
	90	85.4 ($\pm$1.5)	−0.29 ($\pm$0.1)
sAgENM	0	142.7 ($\pm$28)	−1.45 ($\pm$0.3)
	90	144 ($\pm$28)	−1.85 ($\pm$0.1)

2. PGPR viability responses to AgENMs

In terms of viability, PVP-AgENMs were less toxic than ions on a molar basis across all organisms (Fig. 4). Others found ~65 μM PVP-AgENM (10 nm) was required for 50% reduction in viability of *S. meliloti* 1021, whereas we observed an LC₅₀ for AgENM of 207 μM in *S. meliloti* 2011.[35] The large difference in primary particle size used between the studies could explain the differences in observed LC₅₀'s (10 nm vs ~60 nm; smaller nanoparticles are generally more toxic); however, strain specificity in AgENM responses may occur even in the same bacterial species[36] and the exposure medium used was different which can influence the toxicity of ENMs.[37]

The differences in CFUs/ml across test organisms (Table S3) does not completely explain the differences in LC₅₀'s observed. For instance, *S. meliloti* and *P. putida* were both exposed to metals at higher CFUs/mL than *B. amyloliquefaciens*, yet *P. putida* and *B. amyloliquefaciens* exhibited similar LC₅₀'s for AgNO₃ and PVP-AgENM (Table III). *B. subtilis*, which is closely related to *B. amyloliquefaciens*, was generally found in previous studies to be more susceptible than *P. putida* when exposed to uncapped AgENMs; however, viability responses depended on the presence of specific ions (i.e., Ca²⁺, Mg²⁺, Na⁺, K⁺, SO₄²⁻, Cl⁻, HCO₃⁻).[28] A study using a comparable exposure procedure showed ~0.23 μM citrate capped-AgENM (10 nm) was sufficient for nearly complete mortality of *B. subtilis* KACC10111 after 1–2 h of exposure.[30] Another study showed ~300 μM AgENM (32 nm) yielded a ~50% reduction in light emission of *P. putida* BS566::luxCDABE after 1.5 h exposures.[38]

B. amyloliquefaciens and *P. putida* both exhibited significant decreases in % viability starting at 1 μM AgNO₃ and 37 μM PVP-AgENM, with significant reductions continuing with increased concentrations (Fig. 4). Interestingly, both *P. putida* and *B. amyloliquefaciens* viability was reduced by ~30% in response to ~300 μM sAgENM exposure, while there was no significant effect on *S. meliloti* viability (Fig. 4). The observation that *S. meliloti* is generally more resistant to
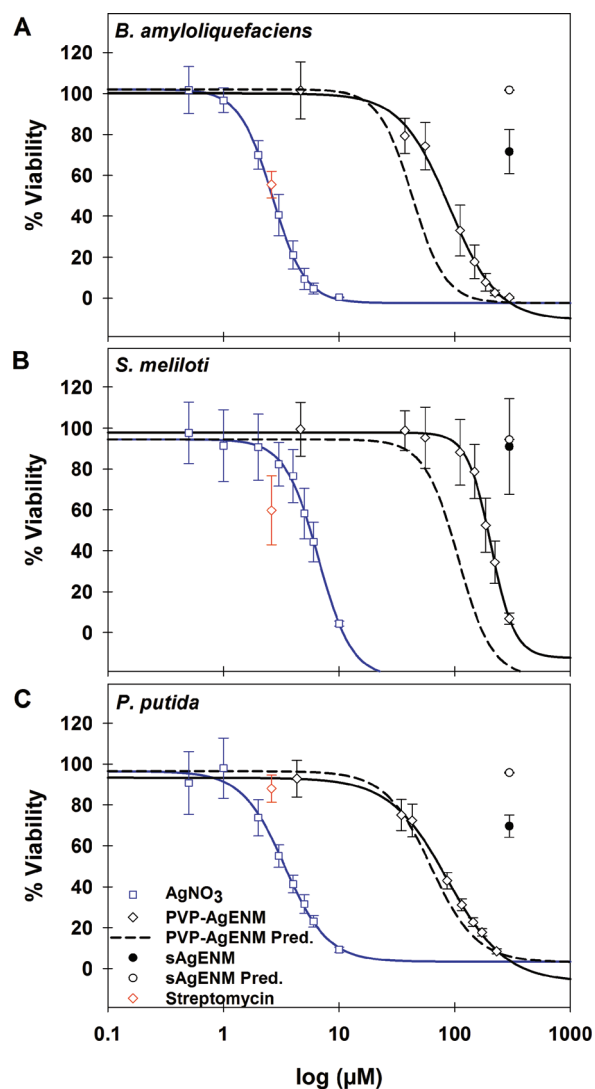

FIG. 4. Viability responses to AgNO₃ (Ag⁺), PVP-AgENM, and sAgENM expressed as percentage of no-metal controls. (a) *B. amyloliquefaciens*, (b) *S. meliloti*, and (c) *P. putida*. Lines represent four-parameter dose response curve fits performed in Sigmaplot. The blue line represents AgNO₃ treatment, the solid black line is PVP-AgENM, and the dotted black line and open circle are predicted response based on abiotic dissolution estimates. Bars are one standard deviation (n = 9). ns = not significant as determined via a Wilcoxon signed rank test (H₀: μ = 100, α 0.05).

Ag⁺, PVP-AgENMs, and sAgENMs has environmental and agricultural implications. In a previous study, we found that amending soil with Ag, Ti, and Zn ENM-containing biosolids significantly inhibited nodulation of *M. truncatula* A17 by *S. meliloti* 2011 but did not reduce *S. meliloti* populations.[17] Results from this study and others[39] suggest silver induced reduction in bacterial viability is likely not the mechanism of toxicity or nodule inhibition.

Coll *et al.*[40] reported predicted no effect concentrations of AgENMs in soil ranging from 40 μmol AgENM/kg to 116 μmol AgENM/kg. Others have found 45 μmol sAgENM/kg (supplied with biosolids amendment) significantly inhibited potential ammonium oxidation activity, with nearly 60% inhibition after 140 days.[41] In the European Union, biosolids amended soils could have AgENM

TABLE III. LC$_{50}$'s of Ag$^+$ and AgENM. LC$_{50}$, the lethal concentration yielding a 50% decrease in viability; PGPR, plant growth promoting rhizobacteria; SE, standard error of regression. LC$_{50}$'s were extrapolated from four-parameter dose response curves in Sigmaplot. Letters (a, b, and c) represent significant differences at $\alpha = 0.05$ using an unpaired t-test with a Bonferroni correction. LC$_{50}$s were compared within treatment (Ag$^+$ or AgENMs).

PGPR	Ag$^+$ LC$_{50}$ (μM $\pm$ SE)	AgENM LC$_{50}$ (μM $\pm$ SE)
B. amyloliquefaciens	2.64 ($\pm$0.1)[a]	89.7 ($\pm$6.3)[a]
S. meliloti	6.62 ($\pm$1.1)[b]	206.5 ($\pm$18)[b]
P. putida	3.39 ($\pm$0.2)[c]	86.4 ($\pm$7.0)[a]

concentrations of approximately 9.3 μmol AgENM/kg by 2020.[5] While it is difficult to directly compare results from liquid culture systems to findings and predictions in soils, we detected responses to AgENMs in liquid cultures that are within the same order of magnitude of predicted near-term environmental concentrations of AgENMs in biosolids amended soils (when comparing mol/kg to molarity).

Predicted free Ag$^+$ activities were higher in PVP-AgENM treatments than AgNO$_3$ treatments, which induced similar reductions in viability (Fig. S3). Accordingly, abiotic dissolution of PVP-AgENM generally over-predicted observed reductions in viability, but correlated well with the observed mortality in *P. putida* (Fig. 4). Abiotic dissolution is only an estimate of the dissolved fraction present during exposure; however, the results suggest the <2 nm fraction likely explains most of the observed response to PVP-AgENM exposures, which agrees with a growing body of literature.[37,42]

Abiotic dissolution estimates under-predicted sAgENM viability responses in *B. amyloliquefaciens* and *P. putida*, implying particle-specific toxicity for these bacteria (Fig. 4). Previously, Colman *et al.*[7] observed shifts in microbial community structure, decreased microbial biomass, and increased N$_2$O production in long-term terrestrial mesocosms treated with AgENM containing biosolids slurries relative to nano-free slurry treatments. The ENM were sulfidized to some degree and the effects of AgENMs were similar or greater than those observed with AgNO$_3$ treatment. This finding, along with ours, shows sulfidation of AgENMs may result in nanospecific delivery of ions leading to prolonged toxicity, likely due to enhanced dissolution at the nano–bio interface. Dissolution at the nano–bio interface has been correlated with toxicity of many ENMs.[37] Additionally, sAgENMs were found to induce phytotoxic effects in the crop plants, *Vigna unguiculata* L. Walp. and *Triticum aestivum*, that were only observed after weeks of exposure,[43] and AgENM enriched biosolids were found to inhibit mycorrhizal-plant associations, including sAgENMs at environmentally relevant concentrations.[6]

Streptomycin reduced cell viability in *S. meliloti* and *B. amyloliquefaciens* by ∼40%–45%, while *P. putida* showed a 10% reduction in viability (Fig. 4). The similarities in viability reduction between *S. meliloti* and *B. amyloliquefaciens* along with the minimal reduction in viability of *P. putida* shows any observed differences in toxicity between the species are not likely purely driven by the differences in cell densities used in this study.

3. PGPR O$_2$ consumption responses

O$_2$ consumption/well of *P. putida* suggests no treatment effect [Fig. 5(c)]; however, O$_2$ consumption-viability plots show that oxygen consumption increased per viable cell under most treatment conditions [Fig. 6(c)]. While it was possible to fit four-parameter curves to *B. amyloliquefaciens* O$_2$ consumption/well measurements [Fig. 5(a)], meaningful four-parameter curve fits for the response in the other organisms were not possible (Fig. 5). The results suggest trends in O$_2$ consumption in response to AgNO$_3$ and PVP-AgENM were specific for the different PGPR tested; with the differences being pronounced when O$_2$ consumption was normalized to viable cell estimates (Fig. 6).

B. amyloliquefaciens generally showed similar increases in O$_2$ consumption in response to AgNO$_3$ and PVP-AgENM
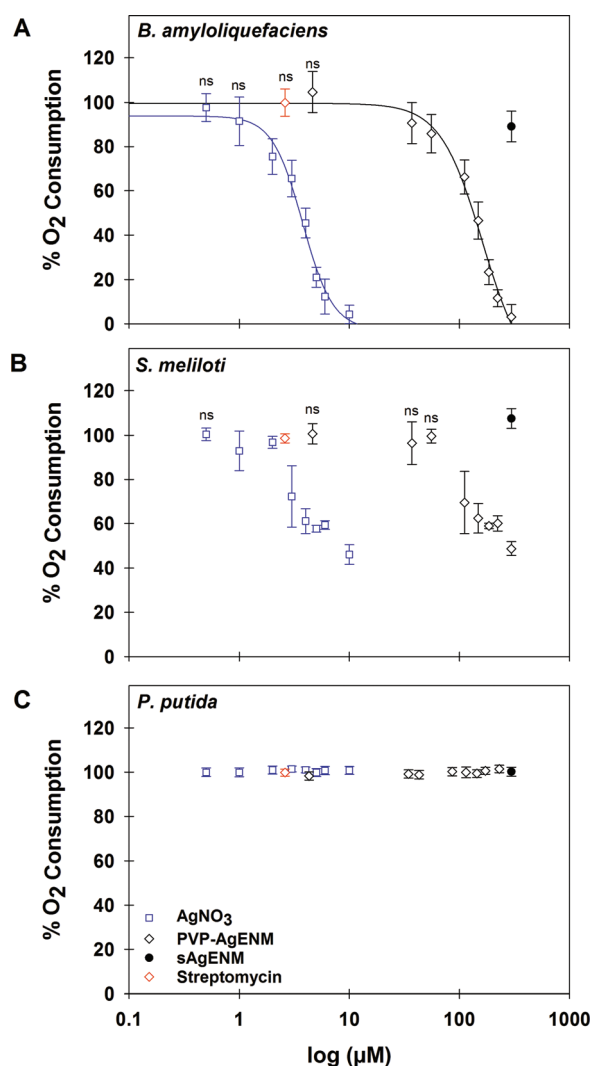

FIG. 5. O$_2$ consumption/well responses of PGPR to Ag$^+$, PVP-AgENM, and sAgENM. O$_2$ consumption/well responses to AgNO$_3$ (Ag$^+$), PVP-AgENM, and sAgENM expressed as percentage of no-metal controls. (a) *B. amyloliquefaciens*, (b) *S. meliloti*, and (c) *P. putida*. Lines represent four-parameter dose response curve fits performed in Sigmaplot. The blue line represents AgNO$_3$ treatment, the solid black line is PVP-AgENM. Bars are one standard deviation ($n = 9$). ns, not significant as determined via Wilcoxon signed rank test (H$_0$: $\mu = 100$, α 0.05).
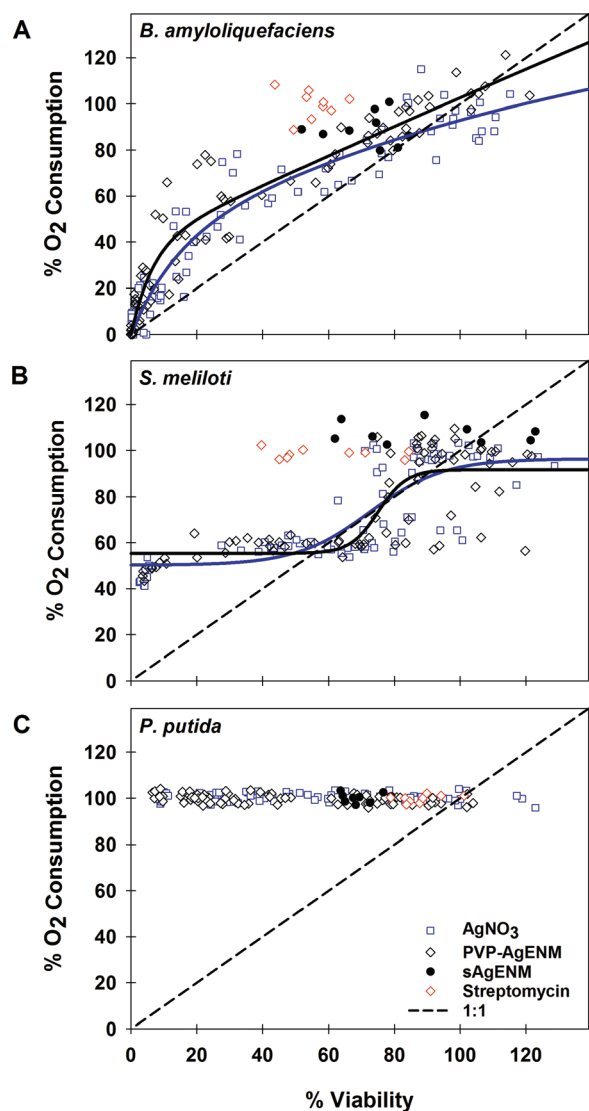
FIG. 6. O₂ consumption-viability responses to AgNO₃ (Ag⁺), PVP-AgENM, and sAgENM expressed as percentage of no-metal controls. (a) *B. amyloliquefaciens*, (b) *S. meliloti*, and (c) *P. putida*. Lines represent regressions performed in Sigmaplot, (a) three-parameter, (b) four-parameter. The blue line represents AgNO₃ treatment, the black line is PVP-AgENM. The dotted line is hypothetical 1:1 relationship between % O₂ consumption and % viability.

exposure, with the effect being exaggerated at <50% viability [Fig. 6(a)]. The trends in O₂ consumption-viability plots of *B. amyloliquefaciens* exposed to AgNO₃ were similar to those from experiment 1, highlighting the reproducibility of the methods across detection platforms. PVP-AgENM and ion exposure of *S. meliloti* also yielded increased O₂ consumption at viable cell densities <50%, but decreased O₂ consumption was observed when % viability was ∼50%–80% [Fig. 6(b)]. PVP-AgENM and ion exposure of *P. putida* yielded increased O₂ consumption at all viable cell densities <100% [Fig. 6(c)]. There was increased O₂ consumption in all PGPR exposed to sAgENM, although the responses were more variable in *S. meliloti* [Fig. 6(b)].

Streptomycin exposure increased O₂ consumption in all PGPR, though the effect was small in *P. putida* (Fig. 6). The

stimulatory effects of streptomycin on bacterial respiration was observed long ago.[44] In our studies, it was a useful treatment for observing increased O₂ consumption, comparing responses across detection platforms, and examining species-specific responses to a medically relevant antibiotic (Fig. 6).

ENMs containing CeO₂, Fe₃O₄, and SnO₂ have been shown to increase respiration as assessed by the metabolic quotient (qCO_2 = basal CO₂ evolution rate/microbial biomass-C) in ENM treated soils in a temporal and spatial (soil horizon) dependent manner.[12] Others have reported decreased respiration in response to Li$_x$Ni$_y$Mn$_z$Co$_{1-y-z}$O₂ containing ENMs in *Shewanella oneidensis* MR-1; however, it is unclear if this is a species-specific response and if respiration responses were normalized for viability responses.[45]

In our study, silver ions and PVP-AgENMs elicited similar respiration responses, which were unique in each of the studied PGPR species. This result, in agreement with others,[36] illustrates the importance of examining the ENM responses of specific bacterial species/strains under identical exposure conditions. Determining the exact biological mechanism of the observed respiration responses was beyond the scope of this study; however, our results are promising for researchers wishing to probe the mechanisms of metabolic responses of bacteria to ENMs, metal ions, and antibiotics.

IV. CONCLUSION

In experiment 1, we developed a high-throughput method of examining O₂ consumption and viability responses in aerobic bacteria. To demonstrate why it is important to account for viable cell numbers in respiration-based toxicity assays, we performed a series of experiments using a variety of substrates pertinent to medical, food, and environmental sciences. The O₂ consumption-viability plots revealed metal specific O₂ consumption responses, with Ag⁺ and streptomycin inducing more pronounced increases in O₂ consumption compared with Zn²⁺ or Ni²⁺. This approach is similar to the metabolic quotient commonly used in ecological research,[46] but different from the bacterial growth efficiency metric previously devised to interpret growth responses in terms of growth and respiration.[47]

In experiment 2, the toxicity of the metals was Ag⁺ > PVP-AgENMs > sAgENMs, from most to least toxic. *S. meliloti* had the highest LC₅₀ for Ag⁺ and PVP-AgENMs, while *P. putida* and *B. amyloliquefaciens* exhibited similar LC₅₀'s. Toxicity of PVP-AgENMs was likely driven by abiotically dissolved silver, while sAgENM toxicity is likely driven by interactions with the cell surface or extracellular milieu. The observed metal and antibiotic specific O₂ consumption responses in *B. amyloliquefaciens* were consistent across two different detection platforms. This finding displays the utility of normalizing respiration responses to viable cell estimates or biomass, which has also been observed by others.[11,12,48] The metal induced species specific respiration responses we observed show the significance of examining toxicity of ENMs and metals to isolated bacterial species/strains. Given the role of microbial respiration in

antibiotic efficacy, the distinct % O_2 consumption-% viability patterns observed in the PGPR in response to Ag^+ and PVP-AgENMs have implications with respect to agricultural application of biosolids and microbial amendments. ENM accumulation in biosolids amended soils is occurring exponentially; concurrently, there has been an increased utilization of microbial amendments for biocontrol of pathogens/pests and to enhance agricultural production. Thus, it is crucial to understand how the distinct respiration responses observed in this study translate to observed toxicity in more realistic scenarios where PGPR and plants are coexposed to AgENMs in test plots.

[1] B. Pan and B. Xing, Eur. J. Soil Sci. **63**, 437 (2012).
[2] F. Gottschalk, T. Sonderer, R. W. Scholz, and B. Nowack, Environ. Sci. Technol. **43**, 9216 (2009).
[3] J. D. Judy and P. M. Bertsch, Adv. Agron. **123**, 1 (2014).
[4] A. E. Pradas del Real *et al.*, Environ. Sci. Technol. **50**, 1759 (2016).
[5] T. Y. Sun, N. A. Bornhöft, K. Hungerbühler, and B. Nowack, Environ. Sci. Technol. **50**, 4701 (2016).
[6] J. D. Judy, J. K. Kirby, C. Creamer, M. J. McLaughlin, C. Fiebiger, C. Wright, T. R. Cavagnaro, and P. M. Bertsch, Environ. Pollut. **206**, 256 (2015).
[7] B. P. Colman *et al.*, PLoS One **8**, e57189 (2013).
[8] G. V. Lowry *et al.*, Environ. Sci. Technol. **46**, 7027 (2012).
[9] M. A. Lobritz, P. Belenky, C. B. Porter, A. Gutierrez, J. H. Yang, E. G. Schwarz, D. J. Dwyer, A. S. Khalil, and J. J. Collins, Proc. Natl. Acad. Sci. **112**, 8173 (2015).
[10] P. Brookes, Biol. Fertil. Soils **19**, 269 (1995).
[11] A. Bérard, C. Mazzia, V. Sappin-Didier, L. Capowiez, and Y. Capowiez, Ecol. Indic. **40**, 27 (2014).
[12] L. Vittori Antisari, S. Carbone, A. Gatti, G. Vianello, and P. Nannipieri, Soil Biol. Biochem. **60**, 87 (2013).
[13] P. Brannen and D. Kenney, J. Ind. Microbiol. Biotechnol. **19**, 169 (1997).
[14] B. Lugtenberg and F. Kamilova, Annu. Rev. Microbiol. **63**, 541 (2009).
[15] A. Gaballa and J. D. Helmann, Biometals **16**, 497 (2003).
[16] C. Galleguillos, C. Aguirre, J. Miguel Barea, and R. Azcón, Plant Sci. **159**, 57 (2000).
[17] C. Chen, J. M. Unrine, J. D. Judy, R. W. Lewis, J. Guo, D. H. McNear, Jr., and O. V. Tsyusko, Environ. Sci. Technol. **49**, 8759 (2015).
[18] J. Duan, W. Jiang, Z. Cheng, J. J. Heikkila, and B. R. Glick, PLoS One **8**, e58640 (2013).
[19] J. D. Brewster, J. Microbiol. Methods **53**, 77 (2003).
[20] R. Hazan, Y.-A. Que, D. Maura, and L. Rahme, BMC Microbiol. **12**, 259 (2012).
[21] D. L. Starnes, J. M. Unrine, C. P. Starnes, B. E. Collin, E. K. Oostveen, R. Ma, G. V. Lowry, P. M. Bertsch, and O. V. Tsyusko, Environ. Pollut. **196**, 239 (2015).
[22] A. R. Whitley, C. Levard, E. Oostveen, P. M. Bertsch, C. J. Matocha, F. von der Kammer, and J. M. Unrine, Environ. Pollut. **182**, 141 (2013).
[23] J. Shaff, B. Schultz, E. Craft, R. Clark, and L. Kochian, Plant Soil **330**, 207 (2010).
[24] D. Wyrzykowski, A. Tesmar, D. Jacewicz, J. Pranczk, and L. Chmurzyński, J. Mol. Recognit. **27**, 722 (2014).
[25] D. Wyrzykowski, B. Pilarski, D. Jacewicz, and L. Chmurzyński, J. Therm. Anal. Calorim. **111**, 1829 (2013).
[26] L. D. Pettit and K. Powell, Chem. Int. **28**, 14 (2006).
[27] K. B. Holt and A. J. Bard, Biochemistry **44**, 13214 (2005).
[28] X. Jin, M. Li, J. Wang, C. Marambio-Jones, F. Peng, X. Huang, R. Damoiseaux, and E. M. Hoek, Environ. Sci. Technol. **44**, 7321 (2010).
[29] A. K. Suresh *et al.*, Environ. Sci. Technol. **44**, 5210 (2010).
[30] S. Kim, Y.-W. Baek, and Y.-J. An, Appl. Microbiol. Biotechnol. **92**, 1045 (2011).
[31] S. W. Kim and Y.-J. An, Appl. Microbiol. Biotechnol. **95**, 243 (2012).
[32] J. D. Van Nostrand, A. G. Sowder, P. M. Bertsch, and P. J. Morris, Environ. Toxicol. Chem. **24**, 2742 (2005).
[33] O. Bondarenko, K. Juganson, A. Ivask, K. Kasemets, M. Mortimer, and A. Kahru, Arch. Toxicol. **87**, 1181 (2013).
[34] D. I. Andersson and D. Hughes, Nat. Rev. Microbiol. **12**, 465 (2014).
[35] N. Joshi, B. T. Ngwenya, and C. E. French, J. Hazard. Mater. **241**, 363 (2012).
[36] J. P. Ruparelia, A. K. Chatterjee, S. P. Duttagupta, and S. Mukherji, Acta Biomater. **4**, 707 (2008).
[37] M.-H. Shen, X.-X. Zhou, X.-Y. Yang, J.-B. Chao, R. Liu, and J.-F. Liu, Sci. Rep. **5**, 9674 (2015).
[38] R. Dams, A. Biswas, A. Olesiejuk, T. Fernandes, and N. Christofi, J. Hazard. Mater. **195**, 68 (2011).
[39] J. D. Judy, J. K. Kirby, M. J. McLaughlin, D. McNear, Jr., and P. M. Bertsch, Environ. Pollut. **214**, 731 (2016).
[40] C. Coll, D. Notter, F. Gottschalk, T. Sun, C. Som, and B. Nowack, Nanotoxicology **10**, 436 (2016).
[41] M. Kraas, K. Schlich, B. Knopf, F. Wege, R. Kägi, K. Terytze, and K. Hund-Rinke, "Long-term effects of sulfidized silver nanoparticles in sewage sludge on soil microflora," Environ. Toxicol. Chem. (published online).
[42] Z.-M. Xiu, Q.-B. Zhang, H. L. Puppala, V. L. Colvin, and P. J. Alvarez, Nano Lett. **12**, 4271 (2012).
[43] P. Wang *et al.*, Nanotoxicology **9**, 1 (2015).
[44] E. L. Oginsky, P. H. Smith, and W. W. Umbreit, J. Bacteriol. **58**, 747 (1949).
[45] M. N. Hang, I. L. Gunsolus, H. Wayland, E. S. Melby, A. C. Mensch, K. R. Hurley, J. A. Pedersen, C. L. Haynes, and R. J. Hamers, Chem. Mater. **28**, 1092 (2016).
[46] T. H. Anderson and K. H. Domsch, Soil Biol. Biochem. **17**, 197 (1985).
[47] P. A. Del Giorgio, J. J. Cole, and A. Cimbleris, Nature **385**, 148 (1997).
[48] S. Drage, D. Engelmeier, G. Bachmann, A. Sessitsch, B. Mitter, and F. Hadacek, J. Microbiol. Methods **88**, 399 (2012).
[49] See supplementary material at http://dx.doi.org/10.1116/1.4995605 for a detailed description of methods, predicted metal activities, colony forming units data, and calibration statistics.

Silver engineered nanomaterials and ions elicit species-specific O$_2$ consumption responses in plant growth promoting rhizobacteria

Ricky W. Lewis, Jason Unrine, Paul M. Bertsch, and David H. McNear